Supporting Information

The Crucial Role of End Group Planarity for Fused-Ring Electron Acceptors in Organic Solar Cells

Jeromy J. Rech, Nicole Bauer, David Dirkes, Joseph Kaplan, Zhengxing Peng, Huotian Zhang, Long Ye, Shubin Liu, Feng Gao, Harald Ade, Wei You[*]

J. J. Rech, N. Bauer, D. Dirkes, J. Kaplan, Prof. W. You
Department of Chemistry, University of North Carolina at Chapel Hill, Chapel Hill, NC 27599, United States
*Email: wyou@unc.edu

Prof. S. Liu
Research Computing Center, University of North Carolina at Chapel Hill, Chapel Hill, North Carolina 27599-3420, United States

Z. Peng, L. Ye, Prof. H. Ade
Department of Physics and Organic and Carbon Electronics Lab (ORaCEL), North Carolina State University, Raleigh, NC 27695, United States

H. Zhang, Prof F. Gao
Biomolecular and Organic Electronics, IFM, Linköping University, Linköping 58183, Sweden

Table of Contents

<u>Literature Survey</u>:

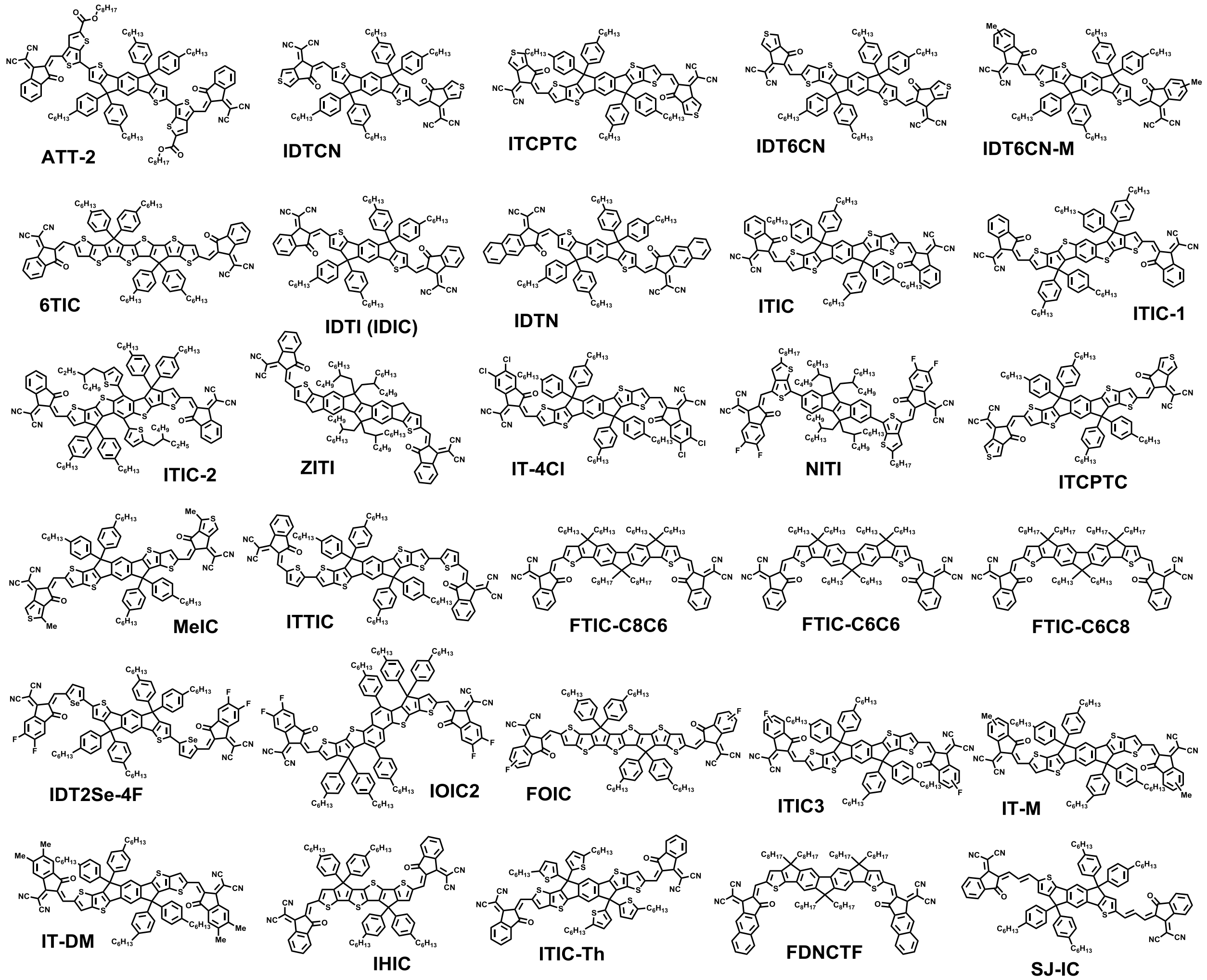

Figure S1 – Chemical structures for each of the various high performance fused-ring electron acceptors (FREAs) used in the literature survey of end-group π-π stacking distances

Table S1 – Literature survey of end-group π-π stacking distances in high performance FREAs

Entry	**FREA**	**PCE (%)**	**π-π stacking distance (Å)**	**Reference**
1	ATT-2	9.58	**3.5**	[1]
2	IDTCN	6.4	**3.53**	[2]
3	ITCPTC	10.74	**3.53**	[2]
4	IDT6CN	9.27	**3.49**	[2]
5	IDT6CN-M	11.20	**3.51**	[2]
6	6TIC	11.07	**3.59**	[3]
7	IDTN	12.2	**3.53**	[4]
8	IDTI (IDIC)	7.4 11.3 6.95	**3.55** **3.52** **3.47**	[4] [24] [26]
9	ITIC	11.41 11.34 10.21	**3.58** **3.5** **3.53**	[5] [8] [15]
10	ITIC-1	8.54	**3.5**	[6]
11	ITIC-2	11.0	**3.5**	[6]
12	ZITI	13.04	**3.43**	[7]
13	IT-4Cl	13.45	**3.51**	[9]
14	NITI	12.74	**3.43**	[10]
15	ITCPTC	11.63	**3.6**	[11]
16	MeIC	12.54	**3.5**	[11]
17	ITTIC	9.12	**3.57**	[12]
18	FTIC-C8C6	10.45	**3.48**	[13]
19	FTIC-C6C6	9.75	**3.45**	[13]
20	FTIC-C6C8	11.12	**3.48**	[13]
21	IDT2Se-4F	11.19	**3.33**	[14]
22	IOIC2	12.3	**3.65**	[16]
23	FOIC	12.0	**3.51**	[17]
24	ITIC3	8.0	**3.49**	[17]
25	IT-M	12.05	**3.5**	[18]
26	IT-DM	11.25	**3.5**	[18]
27	IHIC	10.6 9.77	**3.49** **3.51**	[19] [21]
28	ITIC-Th	8.10 10.9 9.75	**3.51** **3.49** **3.49**	[20] [23] [25]
29	FDNCTF	10.9	**3.4**	[22]
30	SJ-IC	9.27	**3.59**	[26]

Synthesis:

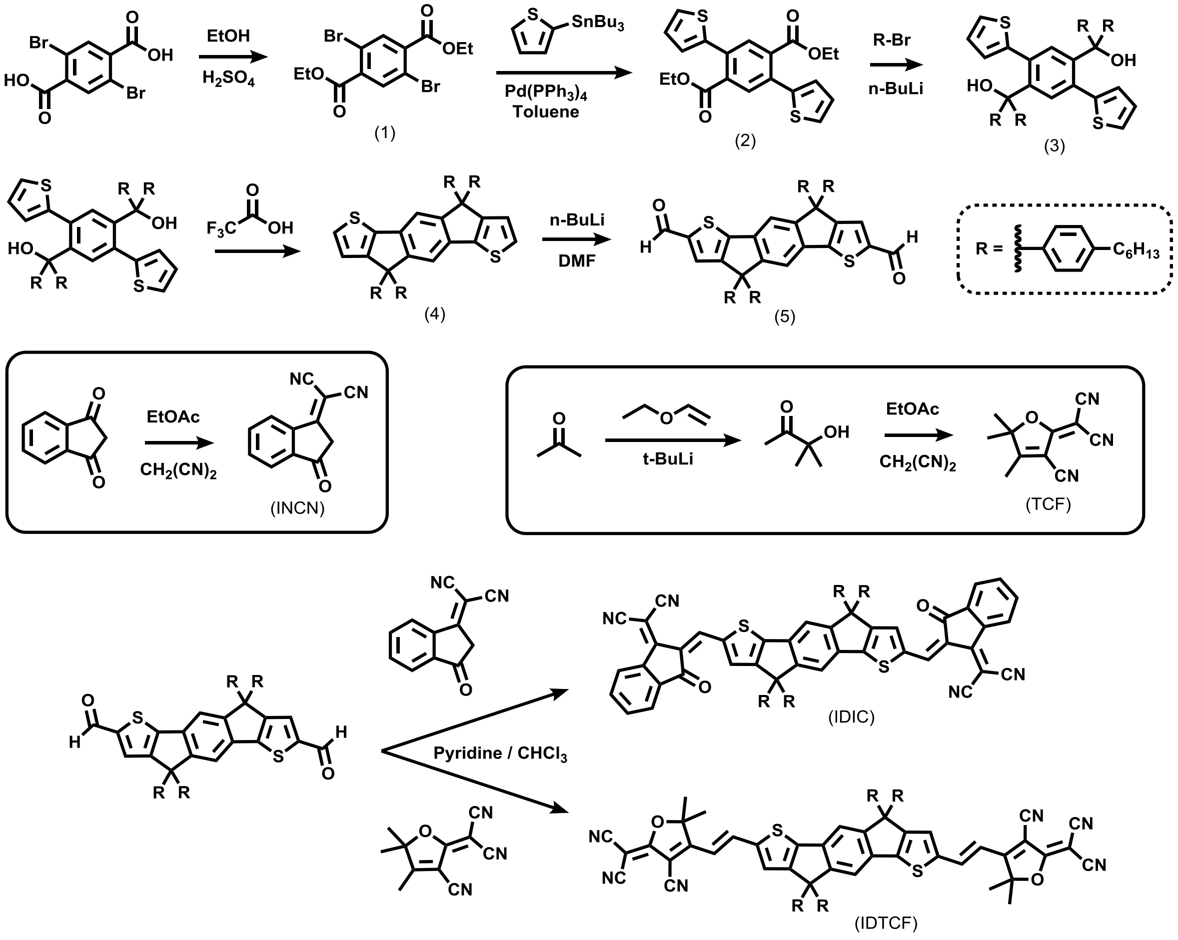

Figure S2 – Reaction scheme for the synthesis of IDIC and IDTCF

All chemicals were purchased from commercial source (Sigma-Aldrich, Fisher, Matrix, etc.) and were used as received except when specified. THF was distilled over sodium and benzophenone before use. For reactions under argon, the glassware was evacuated and refilled with argon for three times and charged with reactants.

Diethyl-2,5-dibromoterephthalate (1)

Commercially available 2,5-dibromoterephthalic acid (1.0 eq, 46.3 mmol) was dissolved in ethanol (400 mL). Concentrated sulfuric acid (4.0 eq, 185.2 mmol) was added, and the resulting mixture was stirred under reflux for 3 days and then cooled to room temperature. The mixture was concentrated via rotary evaporation and run through a short silica plug with DCM as elutent. A white solid was collected after recrystallization in ethanol (yield = 69%). ^{1}H NMR (400 MHz, $CDCl_3$, ppm) δ: 8.02 (s, 2H), 4.42 (q, J=7.14 Hz, 4H), 1.42 (t, J=7.13 Hz, 6H). ^{13}C NMR (101 MHz, $CDCl_3$) δ: 164.07, 136.26, 135.57, 119.91, 62.19, 13.98.

Diethyl-2,5-di(thiophen-2-yl)terephthalate (**2**)

To a solution of diethyl-2,5-dibromoterephthalate (1.0 eq, 10 mmol) and $Pd(PPh_3)_4$ (0.04 eq, 0.37 mmol) in anhydrous toluene (50 mL) was added 2-(tributylstannyl)thiophene (2.2 eq, 22 mmol). The reaction mixture was heated to reflux under argon atmosphere overnight before being cooled to room temperature. The mixture was poured into water (200 mL) and extracted with Et_2O (4 times, 100 mL each). The combined organic phase was washed with water and dried over $MgSO_4$. After concentration, column chromatography (1:1 DCM:hexane) was used to isolate the white solid (yield = 47%). ^{1}H NMR (400 MHz, $CDCl_3$, ppm) δ: 7.83 (s, 2H), 7.41 (dd, J=4.8, 1.4 Hz, 2H), 7.10-7.13 (m, 4H), 4.24 (q, J=7.2 Hz, 4H), 1.18 (t, J=7.2 Hz, 6H). ^{13}C NMR (101 MHz, $CDCl_3$) δ: 167.8, 138.2, 133.7, 133.2, 130.7, 128.6, 128.0, 127.6, 60.9, 14.1.

(2,5-di(thiophen-2-yl))-1,4-phenylene)bis(bis(4-hexylphenyl)methanol) (**3**)

The reactive side chain was first prepared by slowly adding 2.5 M *n*-butyllithium in hexane (5.4 eq, mmol) to a solution of 1-bromo-4-hexylbenzne (5.4 eq, 18.6 mmol) and anhydrous THF (20 mL) at −78 °C. The flask was kept stirring at −78 °C in a dry ice/acetone bath for 2 hours. Diethyl-2,5-di(thiophen-2-yl)terephthalate (1.0 eq, 3.4 mmol) was dissolved in anhydrous THF and the solution was added dropwise, under the protection of argon. The reaction vessel was slowly warmed to room temperature and stirred overnight. The reaction mixture was poured into water and extracted with ethyl acetate (3 times, 50 mL each). The combined organic phase was washed with water and dried over $MgSO_4$. The product was concentrated with rotary evaporation and no further purification was completed to the crude material.

4,4,9,9-tetrakis(4-hexylphenyl)-4,9-dihydro-s-indaceno[1,2-b:5,6-b']dithiophene (**4**)

The crude product of compound 3 was charged into three-neck flask. After adding trifloroacetic acid (0.1 mL) in methylene chloride (10 mL), the mixture was stirred for 1 hours at room temperature. After pouring into water, the mixture was extracted with ethyl acetate (three times, 100 mL each). The combined organic phase was washed with water and dried over $MgSO_4$. After concentration, the resulting crude compound was purified by column chromatography (10:1 hexane:DCM) to give light yellow solid (yield = 60%). ^{1}H NMR (400 MHz, $CDCl_3$, ppm) δ: 7.42 (s, 2H), 7.23 (d, J=4.9 Hz, 2H), 7.15 (d, J=8.3 Hz, 8H), 7.04 (d, J=8.3 Hz, 8H), 6.99 (d, J=4.9 Hz, 2H), 2.59 – 2.50 (m, 8H), 1.37 – 1.24 (m, 28H), 0.91 – 0.83 (m, 4H). ^{13}C NMR (101 MHz, $CDCl_3$) δ: 156.05, 153.60, 142.81, 141.89, 141.68, 135.65, 128.48, 128.08, 127.72, 123.23, 117.69, 62.45, 35.39, 31.56, 31.16, 28.98, 22.43, 13.92.

4,4,9,9-tetrakis(4-hexylphenyl)-4,9-dihydro-s-indaceno[1,2-b:5,6-b']dithiophene-2,7-dicarbaldehyde (**5**)

In a dry round-bottomed flask, compound 4 (1.0 eq, 0.14 mmol) was dissolved in anhydrous THF (25 mL) and placed under an argon atmosphere. The solution was cooled to −78 °C with a dry ice/acetone bath and stirred while 2.5 M *n*-butyllithium in hexane (2.6 eq, 0.36 mmol) was added dropwise. The mixture was stirred for one hour at −78 °C, and then anhydrous DMF (10.0 eq, 1.38 mmol) was added dropwise. The reactant was warmed to room temperature and stirred overnight. The reaction mixture was poured into water (100 mL) and extracted with DCM (5 times, 50 mL each). The combined organic phases where washed with water and dried with $MgSO_4$ and concentrated. The resulting crude compound was purified by column chromatography (3:2 hexane:DCM) to give a yellow solid (yield = 61%). ^1H NMR (400 MHz, $CDCl_3$, ppm) δ: 9.83 (s, 2H), 7.65 (s, 2H), 7.59 (s, 2H), 7.11 (m, 16H), 2.56 (t, J=7.7 Hz, 8H), 1.62–1.53 (m, 8H), 1.36–1.26 (m, 24H), 0.87 (t, J=6.9 Hz, 12H). ^{13}C NMR (101 MHz, $CDCl_3$) δ: 182.52, 156.67, 154.87, 150.12, 145.94, 141.79, 140.21, 135.44, 131.65, 128.47, 127.48, 118.33, 62.34, 35.38, 31.53, 31.13, 28.93, 22.42, 13.91.

2-(3-oxo-2,3-dihydro-1H-inden-1-ylidene)malononitrile (**INCN**)

Indane-1,3-dione (1.0 eq, 13.7 mmol) and malononitrile (2.0 eq, 27.4 mmol) were dissolved in absolute ethanol (35 mL), and then anhydrous sodium acetate (1.3 eq, 17.8 mmol) was added while stirring. After 50 min, the mixture was poured into cold water (400 mL), and acidified to pH 1–2 by addition of the hydrochloric acid. The precipitate was filtered and recrystallized from glacial acetic acid (yield = 76%). ^1H NMR (400 MHz, $CDCl_3$, ppm) δ: 8.66 (d, J=7.8 Hz, 1H), 7.99 (m, 2H), 7.83-7.92 (m, 2H), 2.09 (s, 2H). ^{13}C NMR (101 MHz, $CDCl_3$) δ: 194.18, 165.69, 135.13, 125.51, 1.24.20, 111.48, 111.57, 78.67, 42.70.

2-(3-cyano-4,5,5-trimethylfuran-2(5H)-ylidene)malononitrile (**TCF**)

Ethyl vinyl ether (1.4 eq, 14 mmol) was added to anhydrous THF (30 mL) under the protection of argon. The mixture was cooled to −78 °C with a dry ice/acetone bath and stirred while 2.0 M *tert*-butyllithium in heptane (1.2 eq, 12 mmol) was slowly added dropwise. The reaction mixture was warmed to room temperature for 30 minutes, then cooled back to −78 °C with a dry ice/acetone bath. Dry acetone (1.0 eq, 10 mmol) was added via syringe and the reaction mixture was allowed to slowly warm to room temperature overnight. A 20 mL mixture of 1:1 methanol:water was added dropwise and then followed with 2 mL of concentrated HCl. The reaction mixture was stirred under the protection of argon for 2 hours. Afterwards, the reaction mixture was concentrated to orange oil. No further purification steps where done on the hydroxy-ketone species. In a dry round bottom flask, malononitrile (2.0 eq, 20 mmol) and sodium ethoxide (1.0 eq, 10 mmol) where dissolved in anhydrous ethanol (30 mL) under the protection of argon. After stirring for 2 hours, the crude product was added and the reaction mixture stirred overnight. The reaction mixture was concentrated to a dark orange sludge, which was neutralized with 6 M HCl (10 mL). The crude product was washed with water (10 mL) and collected via filtration. The pale yellow solid was washed with minimal amounts of water and dried in the oven overnight (yield = 66%). ^1H NMR (400 MHz, $CDCl_3$, ppm) δ: 2.36 (s, 3H), 1.63 (s, 6H). ^{13}C NMR (101 MHz, $CDCl_3$) δ: 182.48, 175.15, 110.99, 110.36, 108.94, 104.83, 99.73, 24.39, 14.19.

2,2'-((2Z,2'Z)-((4,4,9,9-tetrakis(4-hexylphenyl)-4,9-dihydro-s-indaceno[1,2-b:5,6-b']dithiophene-2,7-diyl)bis(methaneylylidene))bis(3-oxo-2,3-dihydro-1H-indene-2,1-diylidene))dimalononitrile (IDIC)

INCN (6.9 eq, 0.38 mmol) was added into the mixture of compound 5 (1.0 eq, 0.06 mmol) in chloroform (15 mL) and pyridine (0.5 mL) mixture; the reactant was purged with argon for 30 min and then refluxed overnight. After cooling to room temperature, the reaction was poured into methanol and the precipitate was filtered off. The crude product was purified by column chromatography (2:1 chloroform:hexane) to give a metallic purple solid (yield = 75%). ^{1}H NMR (400 MHz, $CDCl_3$, ppm) δ: 8.90 (s, 2H), 8.69 (d, J=8.0 Hz, 2H), 7.92 (d, J=7.1 Hz, 2H), 7.80 – 7.69 (m, 8H), 7.16 – 7.09 (m, 16H), 2.58 (t, J=7.9 Hz, 8H), 1.60 (m, 8H), 1.32 – 1.26 (m, 24H), 0.90 – 0.86 (m, 12H). ^{13}C NMR (101 MHz, $CDCl_3$) δ: 188.21, 180.83, 160.42, 158.92, 157.79, 157.77, 142.19, 141.30, 140.15, 138.30, 136.93, 136.71, 135.07, 134.36, 128.61, 127.47, 69.28, 62.82, 35.39, 31.55, 31.13, 29.54, 28.91, 22.42, 13.93. Mass Spec: $C_{90}H_{83}N_4O_2S_2$ $[M+H]^+$, *m/z* = 1315.59157, mass error = –2.8 ppm.

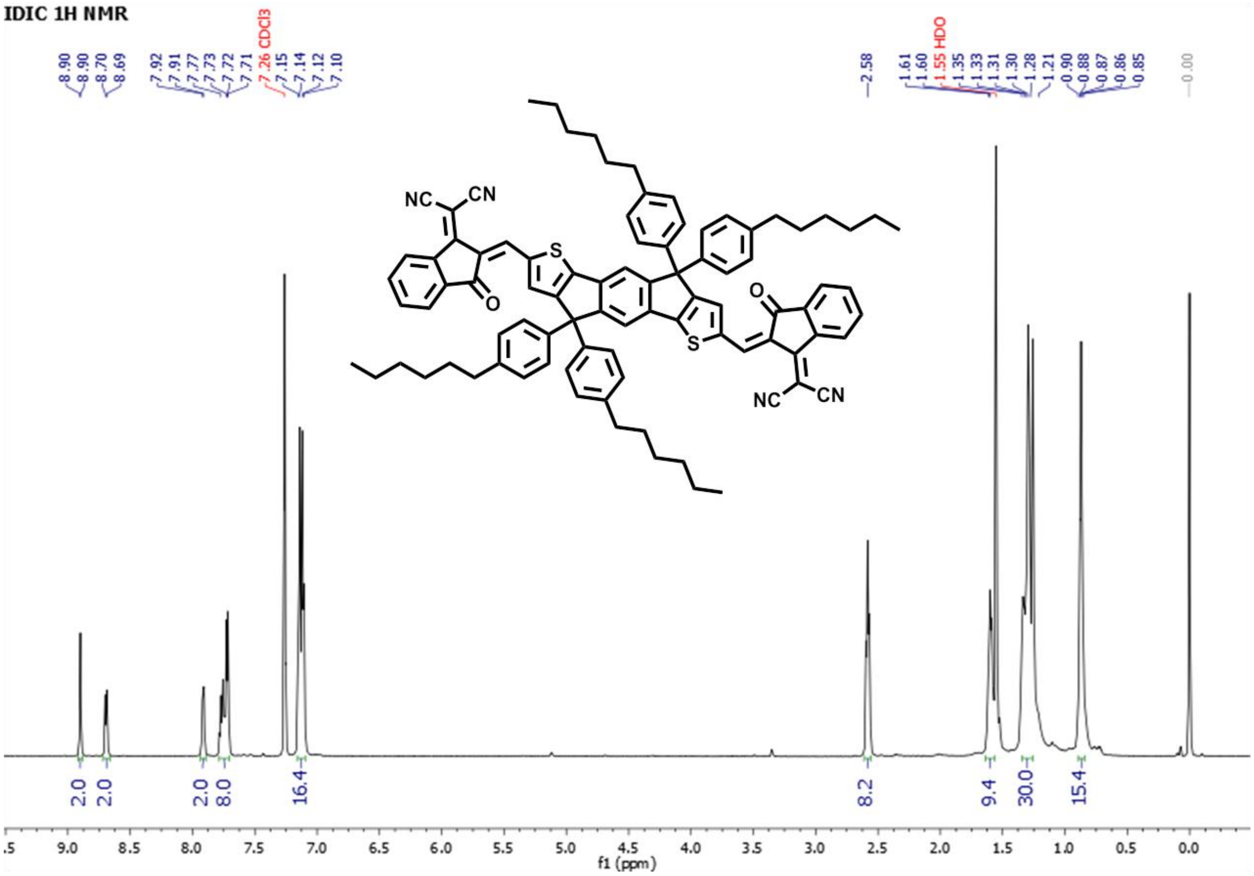

Figure S3 – 1H NMR for IDIC

2,2'-(((1E,1'E)-(4,4,9,9-tetrakis(4-hexylphenyl)-4,9-dihydro-s-indaceno[1,2-b:5,6-b']dithiophene-2,7-diyl)bis(ethene-2,1-diyl))bis(3-cyano-5,5-dimethylfuran-4(5H)-yl-2(5H)-ylidene))dimalononitrile (IDTCF)

TCF (6.9 eq, 0.38 mmol) was added into the mixture of compound 5 (1.0 eq, 0.06 mmol) in chloroform (5 mL) and pyridine (15 mL) mixture; the reactant was purged with argon for 30 min and then refluxed for 48 hours. After cooling to room temperature, the reaction was poured into methanol and the precipitate was filtered off. The crude product was purified by column chromatography (chloroform eluting) to give a blue-purple solid (yield = 52%). ^{1}H NMR (400 MHz, CDCl$_3$, ppm) δ: 7.76 (d, J=15.9 Hz, 2H), 7.53 (s, 2H), 7.38 (s, 2H), 7.10 (m, 16H), 6.66 (d, J=15.8 Hz, 2H), 2.57 (t, J=7.8 Hz, 8H), 1.73 (s, 12H), 1.60 (m, 8H), 1.25 – 1.37 (m, 24H), 0.87 (t, J=6.9 Hz, 12H). ^{13}C NMR (101 MHz, CDCl$_3$) δ: 194.12, 162.82, 144.95, 140.17, 138.21, 136.90, 134.71, 130.64, 128.77, 127.60, 94.66, 92.37, 69.14, 66.19, 50.20, 35.56, 31.70, 31.34, 29.10, 26.25, 22.60, 18.60, 14.10. Mass Spec: C$_{88}$H$_{89}$N$_6$O$_2$S$_2$ [M+H]$^+$, *m/z* = 1325.64624, mass error = –1.5 ppm.

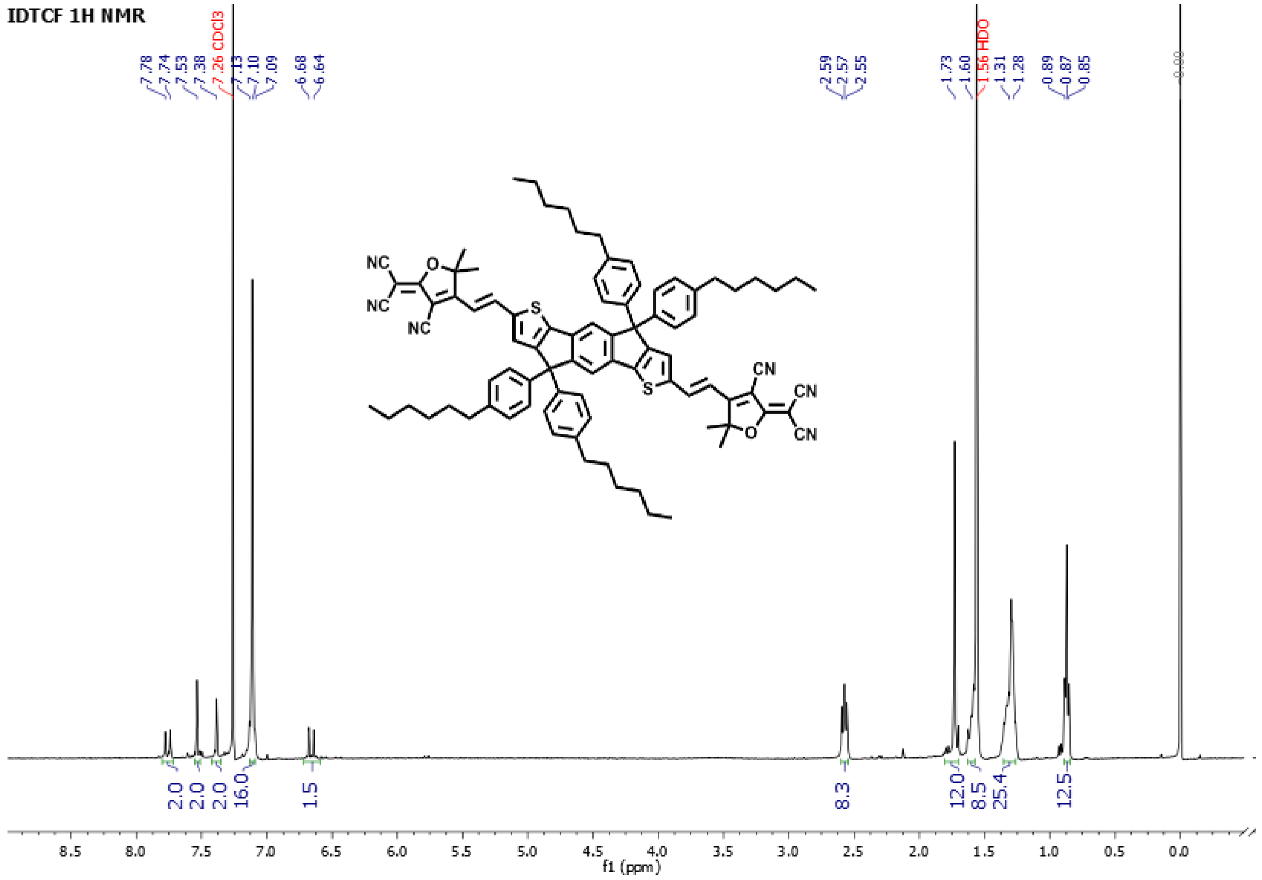

Figure S4 – 1H NMR for IDTCF

Characterization Methods:

1H and 13C nuclear magnetic resonance (NMR) measurements were recorded with Bruker DRX spectrometers (400 MHz). Mass Spectrometry was run on a ThermoScientific Q Exactive HF-X mass spectrometer and analyzed via Xcalibur (ThermoFisher). UV-Visible absorption spectra were obtained with a Shimadzu UV-2600 spectrophotometer. A Rigaku SmartLab was used for high-resolution X-ray diffractometer (XRD) measurements.

CV measurements were carried out on thin films using a Bioanalytical Systems (BAS) Epsilon potentiostat with a standard three-electrode configuration. A three electrode cell of a glassy carbon working electrode, Ag/Ag^+ reference electrode, and Pt counter electrode were used. Films of the FREAs were drop-cast onto the glassy carbon electrode from hot chloroform solution (2 mg/mL, with tetrabutylammonium hexafluorophosphate added at 100 wt%) and dried using a heat gun. 0.1 M solution of tetrabutylammonium hexafluorophosphate in anhydrous acetonitrile was used as a supporting electrolyte. Scans were carried out under argon atmosphere at a scan rate of 100 mV/s. The reference electrode was calibrated using a ferrocene/ferrocenium redox couple.

Solar cell devices were tested under AM 1.5G irradiation calibrated with an NREL certified standard silicon solar cell. Current density-voltage curves were measured via a Keithley 2400 digital source meter.

GIWAXS measurements were performed at beamline 7.3.3 [Ref 27] at the ALS. The 10 KeV X-ray beam was incident at a grazing angle of 0.13 degree. The scattered X-rays were detected using a 2D area detector (Pilatus 1M). All measurements were conducted under He atmosphere to reduce air scattering.

Device Fabrication:

Solar cells were fabricated on glass substrates with patterned indium doped tin oxide (ITO). ITO substrates were cleaned via sonication in deionized water, acetone and isopropyl alcohol for fifteen minutes each, followed by UV-ozone treatment for 15 minutes. The ZnO precursor solution was prepared by dissolving 1 g of zinc acetate dihydrate and 0.28 g of ethanolamine in 10 mL of 2-methoxyethanol. The solution was stirred overnight, and then spun cast onto the cleaned ITO at 4000 rpm for 30 s, then baked at 150°C for 30 minutes in air. The substrates were then transferred into a nitrogen filled glovebox. FTAZ:Acceptor solutions (FTAZ:IDIC or IDTCF=1:1, 6 mg/mL FTAZ) in chlorobenzene were prepared and spuncast onto the ZnO. The solar cells were finished by evaporation of 10 nm MoO_3 and 70 nm of aluminum, with a device area of 13 mm^2.

Table S2 – Photovoltaic characteristics of the FTAZ:IDIC and FTAZ:IDTCF solar cells in various different solvents [CF = chloroform; CB = chlorobenzene; Tol = toluene].

Acceptor	Solvent	J_{sc} (mA/cm^2)	V_{oc} (V)	FF (%)	PCE (%)
IDIC	CF	7.48 ± 0.19	0.876 ± 0.004	40.9 ± 1.1	2.68 ± 0.06
	CB	10.79 ± 0.18	0.954 ± 0.004	50.6 ± 1.5	5.21 ± 0.19
	Tol	8.29 ± 0.81	0.944 ± 0.008	43.1 ± 1.0	3.37 ± 0.33
IDTCF	CF	1.51 ± 0.11	0.738 ± 0.008	39.9 ± 0.4	0.44 ± 0.04
	CB	2.10 ± 0.12	0.705 ± 0.034	39.6 ± 1.8	0.59 ± 0.06
	Tol	1.25 ± 0.10	0.737 ± 0.009	41.5 ± 0.6	0.38 ± 0.03

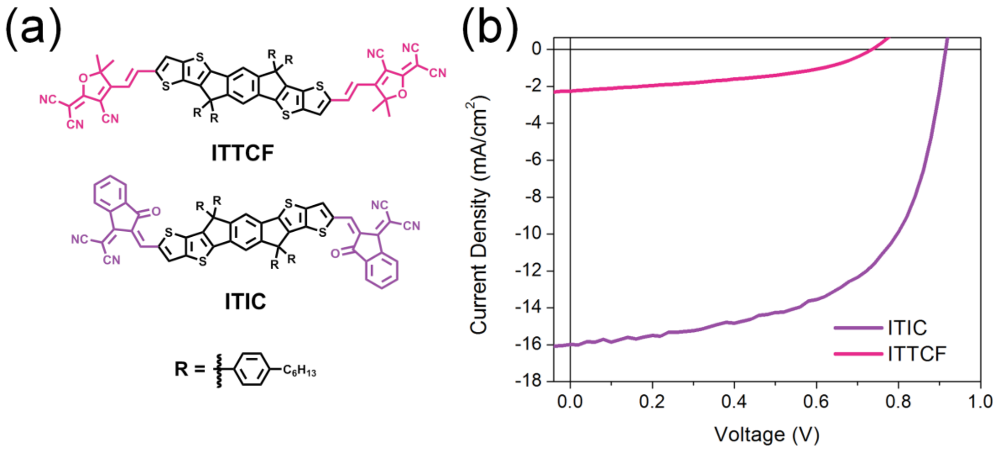

Figure S5 – (a) Chemical structure for ITIC and ITTCF electron acceptors and (b) representative JV curve for each acceptor paired with FTAZ

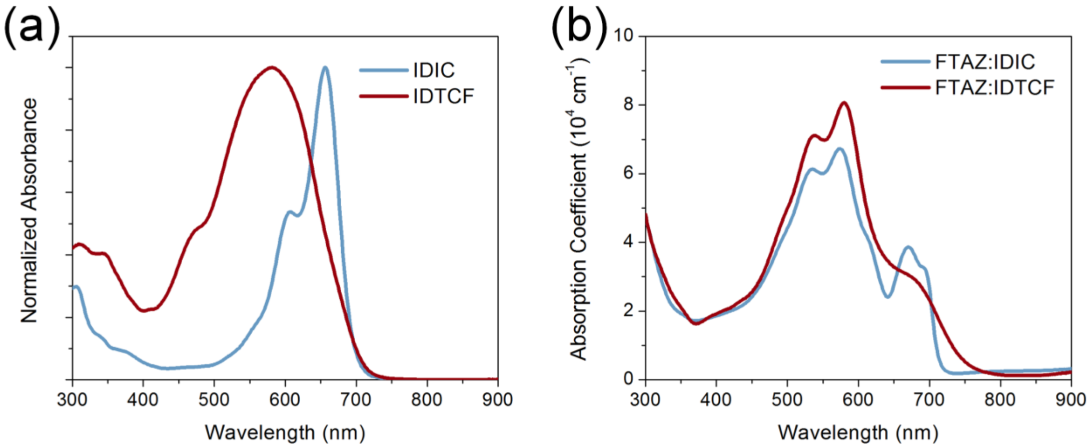

Figure S6 – (a) Dilute solution UV-Vis for each FREA dissolved in chloroform and (b) full device absorption coefficient for each FTAZ:FREA blend

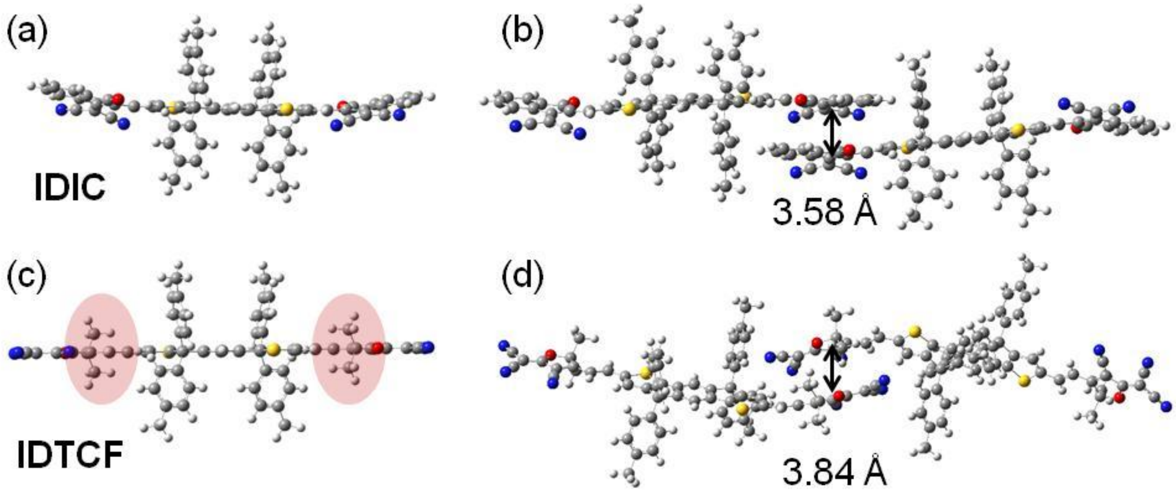

Figure S7 – Minimized energy conformation for (a) IDIC unit, (b) IDIC dimer, (c) IDTCF unit, and (d) IDTCF dimer. Additionally, the closest packing of the FREAs was shown to be (b) 3.58 Å for IDIC and (d) 3.84 Å for IDTCF

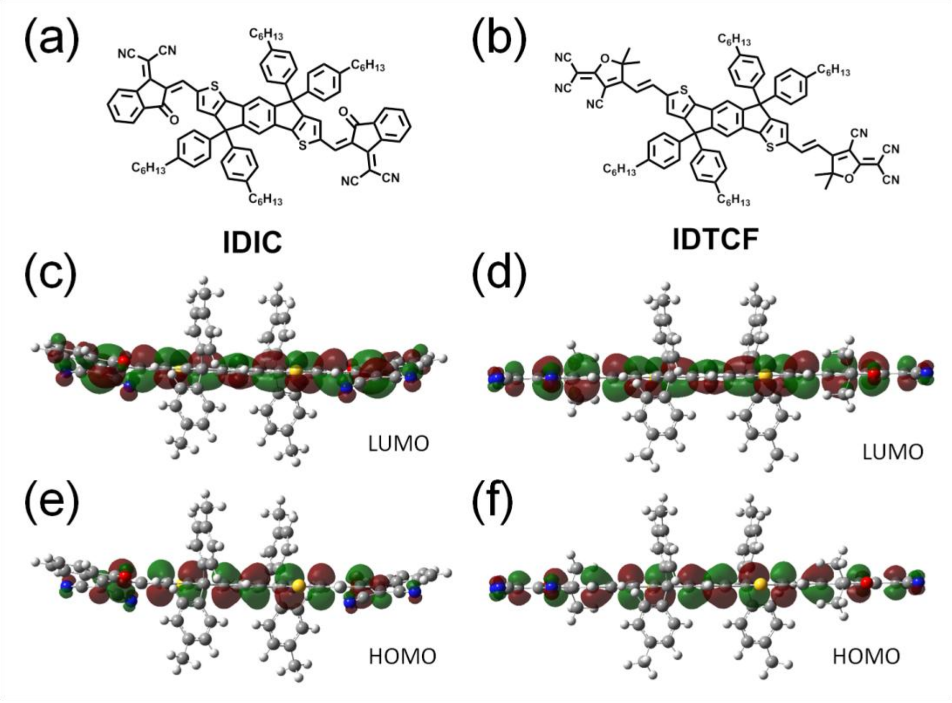

Figure S8 – Chemical structure of (a) IDIC and (b) IDTCF, including the (c) LUMO and (e) HOMO of IDIC next to the (d) LUMO and (f) HOMO of IDTCF

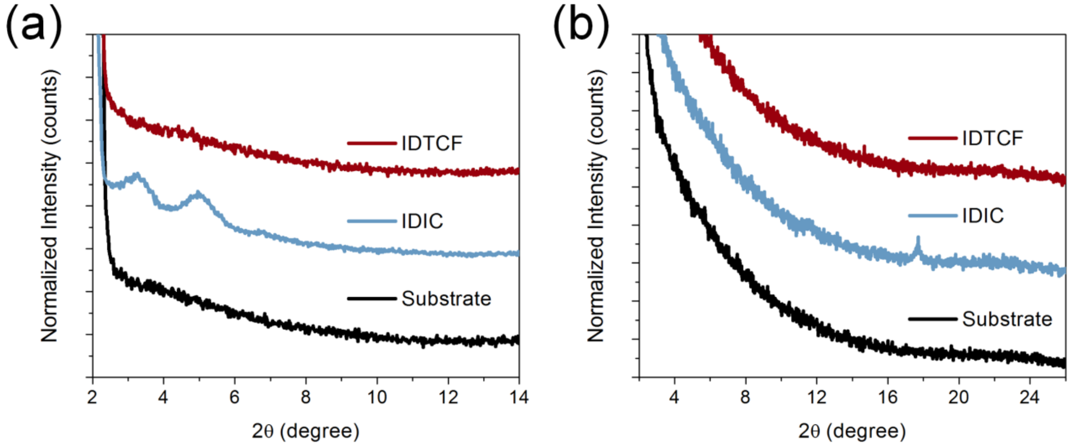

Figure S9 – (a) Out-of-plane and (b) in-plane XRD scattering spectra for each acceptor, including blank substrate

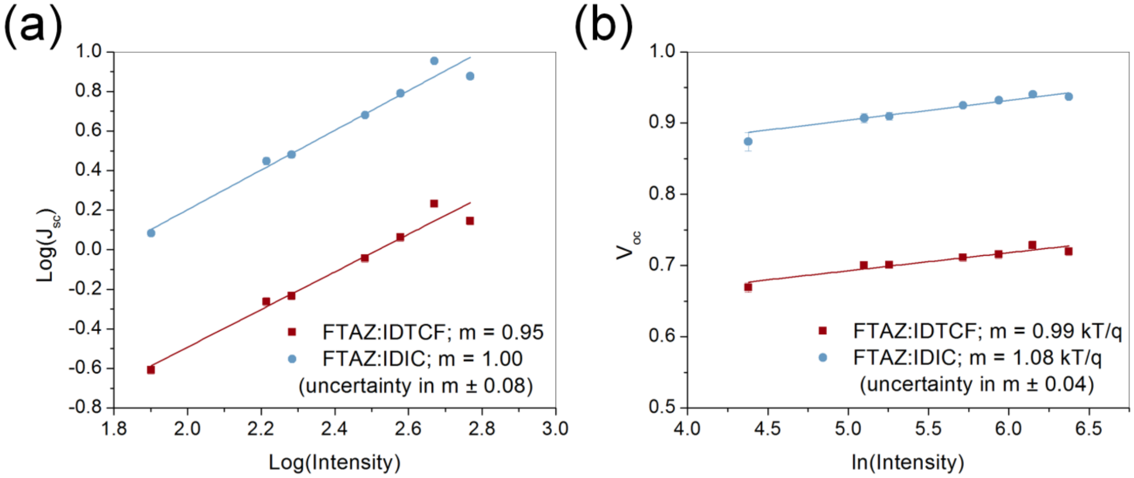

Figure S10 – Light intensity dependence of (a) short-circuit current and (b) open-circuit voltage for both FTAZ:IDIC and FTAZ:IDTCF blends

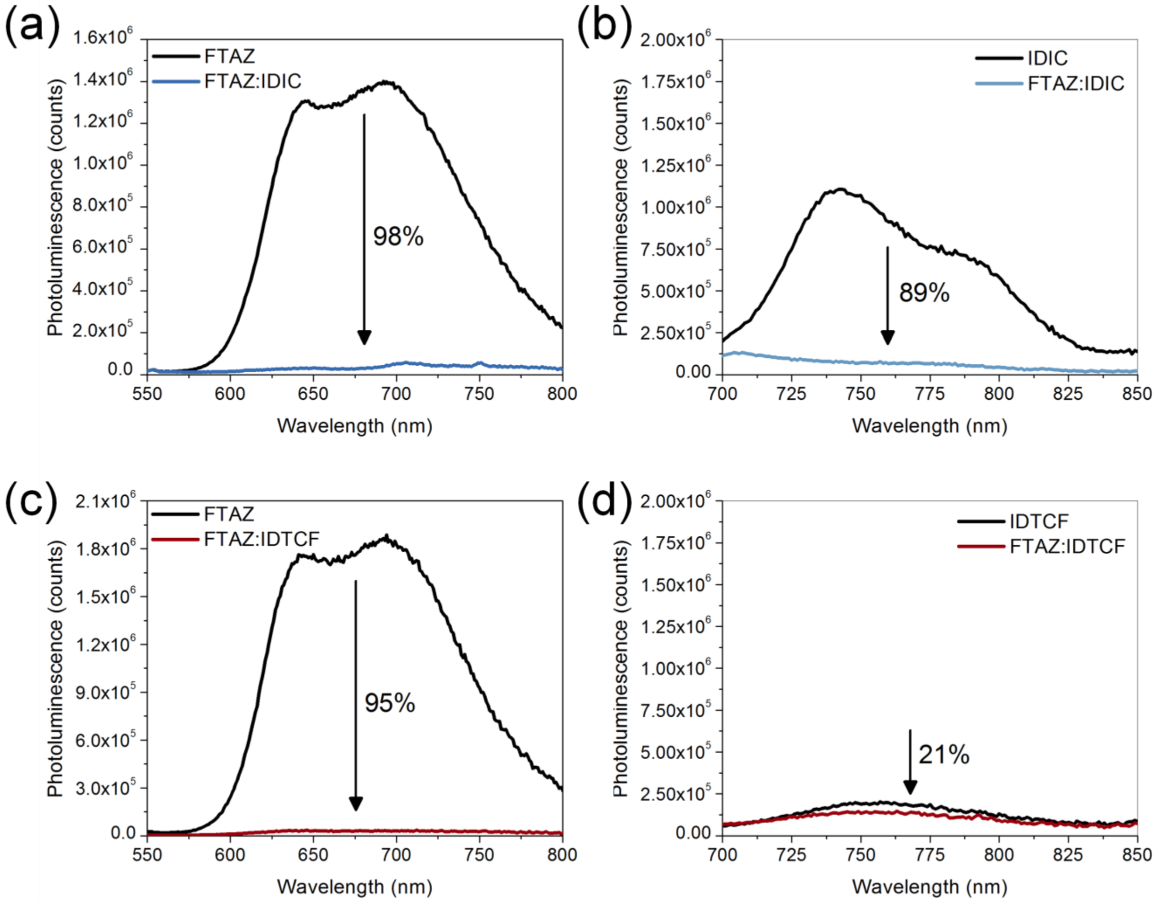

Figure S11 – (a) Photoluminescence (PL) of neat FTAZ and FTAZ:IDIC blend films excited at 500 nm, (b) PL of neat IDIC and FTAZ:IDIC blend films excited at 650 nm, (c) PL of neat FTAZ and FTAZ:IDTCF blend films excited at 480 nm, (d) PL of neat IDTCF and FTAZ:IDTCF blend films excited at 650 nm

Table S3 – Photoluminescence Quantum Efficiency (PLQE) Summary – excited at 532 nm

	FTAZ:IDIC	**FTAZ:IDTCF**	**FTAZ**	**IDIC**	**IDTCF**
PLQE	0.0%	0.4%	0.3%	3.3%	3.0%

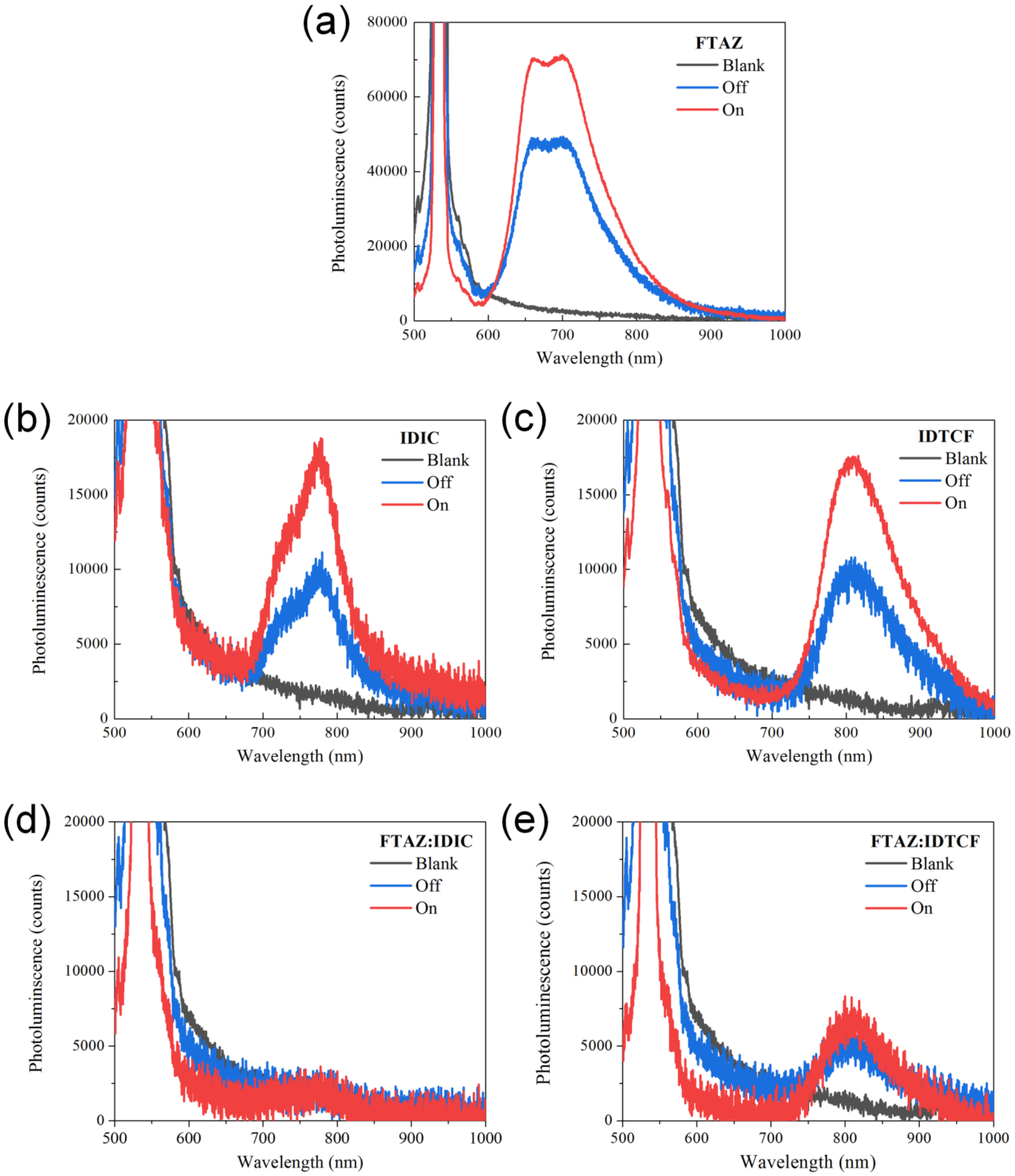

Figure S12 – (a) PL spectra of neat FTAZ excited at 532 nm, (b) PL spectra of neat IDIC excited at 532 nm, (c) PL spectra of neat IDTCF excited at 532 nm, (d) PL spectra of FTAZ:IDIC blend film excited at 532 nm, (e) PL spectra of FTAZLIDTCF excited at 532 nm

Note: Quantifying PLQE requires three measurements: (1) in the ***blank*** experiment the laser is directed into the integrating sphere with no sample mounted (2) in the ***off*** experiment the sample is excited indirectly by the light scattered from the integrating sphere wall (3) in the ***on*** experiment the sample is excited directly by the laser beam

References:

1. Liu, F.; Zhou, Z.; Zhang, C.; Zhang, J.; Hu, Q.; Vergote, T.; Liu, F.; Russell, T. P.; Zhu, X. Efficient Semitransparent Solar Cells with High NIR Responsiveness Enabled by a Small-Bandgap Electron Acceptor. *Adv. Mater.* **2017**, *29*, 1606574.
2. Gao, W.; Zhang, M.; Liu, T.; Ming, R.; An, Q.; Wu, K.; Xie, D.; Luo, Z.; Zhong, C.; Liu, F.; et al. Asymmetrical Ladder-Type Donor-Induced Polar Small Molecule Acceptor to Promote Fill Factors Approaching 77% for High-Performance Nonfullerene Polymer Solar Cells. *Adv. Mater.* **2018**, *30*, 1800052.
3. Shi, X.; Chen, J.; Gao, K.; Zuo, L.; Yao, Z.; Liu, F.; Tang, J.; Jen, A. K.-Y. Terthieno[3,2- b]Thiophene (6T) Based Low Bandgap Fused-Ring Electron Acceptor for Highly Efficient Solar Cells with a High Short-Circuit Current Density and Low Open-Circuit Voltage Loss. *Adv. Energy Mater*. **2018**, *8*, 1702831.
4. Li, S.; Ye, L.; Zhao, W.; Liu, X.; Zhu, J.; Ade, H.; Hou, J. Design of a New Small-Molecule Electron Acceptor Enables Efficient Polymer Solar Cells with High Fill Factor. *Adv. Mater.* **2017**, *29*, 1704051.
5. Bin, H.; Gao, L.; Zhang, Z.-G.; Yang, Y.; Zhang, Y.; Zhang, C.; Chen, S.; Xue, L.; Yang, C.; Xiao, M.; et al. 11.4% Efficiency Non-Fullerene Polymer Solar Cells with Trialkylsilyl Substituted 2D-Conjugated Polymer as Donor. *Nat. Commun.* **2016**, *7*, 13651.
6. Wang, J.; Wang, W.; Wang, X.; Wu, Y.; Zhang, Q.; Yan, C.; Ma, W.; You, W.; Zhan, X. Enhancing Performance of Nonfullerene Acceptors via Side-Chain Conjugation Strategy. *Adv. Mater*. **2017**, *29*, 1702125.
7. Liu, W.; Zhang, J.; Zhou, Z.; Zhang, D.; Zhang, Y.; Xu, S.; Zhu, X. Design of a New Fused-Ring Electron Acceptor with Excellent Compatibility to Wide-Bandgap Polymer Donors for High-Performance Organic Photovoltaics. *Adv. Mater.* **2018**, *30*, 1800403.
8. Zheng, Z.; Awartani, O. M.; Gautam, B.; Liu, D.; Qin, Y.; Li, W.; Bataller, A.; Gundogdu, K.; Ade, H.; Hou, J. Efficient Charge Transfer and Fine-Tuned Energy Level Alignment in a THF-Processed Fullerene-Free Organic Solar Cell with 11.3% Efficiency. *Adv. Mater.* **2017**, *29*, 1604241.
9. Zhang, H.; Yao, H.; Hou, J.; Zhu, J.; Zhang, J.; Li, W.; Yu, R.; Gao, B.; Zhang, S.; Hou, J. Over 14% Efficiency in Organic Solar Cells Enabled by Chlorinated Nonfullerene Small-Molecule Acceptors. *Adv. Mater.* **2018**, *30*, 1800613.
10. Xu, S. jie; Zhou, Z.; Liu, W.; Zhang, Z.; Liu, F.; Yan, H.; Zhu, X. A Twisted Thieno[3,4- b]Thiophene-Based Electron Acceptor Featuring a 14-π-Electron Indenoindene Core for High-Performance Organic Photovoltaics. *Adv. Mater.* **2017**, *29*, 1704510.
11. Luo, Z.; Bin, H.; Liu, T.; Zhang, Z.-G.; Yang, Y.; Zhong, C.; Qiu, B.; Li, G.; Gao, W.; Xie, D.; et al. Fine-Tuning of Molecular Packing and Energy Level through Methyl Substitution Enabling Excellent Small Molecule Acceptors for Nonfullerene Polymer Solar Cells with Efficiency up to 12.54%. *Adv. Mater.* **2018**, *30*, 1706124.
12. Zhang, Z.; Liu, W.; Rehman, T.; Ju, H.; Mai, J.; Lu, X.; Shi, M.; Zhu, J.; Li, C.-Z.; Chen, H. Energy-Level Modulation of Non-Fullerene Acceptors to Achieve High-Efficiency Polymer Solar Cells at a Diminished Energy Offset. *J. Mater. Chem. A* **2017**, *5*, 9649–9654.
13. Zhang, Z.; Li, M.; Liu, Y.; Zhang, J.; Feng, S.; Xu, X.; Song, J.; Bo, Z. Simultaneous Enhancement of the Molecular Planarity and the Solubility of Non-Fullerene Acceptors: Effect of Aliphatic Side-Chain Substitution on the Photovoltaic Performance. *J. Mater. Chem. A* **2017**, *5*, 7776–7783.

14. Liang, Z.; Li, M.; Zhang, X.; Wang, Q.; Jiang, Y.; Tian, H.; Geng, Y. Near-Infrared Absorbing Non-Fullerene Acceptors with Selenophene as π Bridges for Efficient Organic Solar Cells. *J. Mater. Chem. A* **2018**, *6*, 8059–8067.
15. Zhang, Z.; Yu, J.; Yin, X.; Hu, Z.; Jiang, Y.; Sun, J.; Zhou, J.; Zhang, F.; Russell, T. P.; Liu, F.; et al. Conformation Locking on Fused-Ring Electron Acceptor for High-Performance Nonfullerene Organic Solar Cells. *Adv. Funct. Mater.* **2018**, *28*, 1705095.
16. Zhu, J.; Ke, Z.; Zhang, Q.; Wang, J.; Dai, S.; Wu, Y.; Xu, Y.; Lin, Y.; Ma, W.; You, W.; et al. Naphthodithiophene-Based Nonfullerene Acceptor for High-Performance Organic Photovoltaics: Effect of Extended Conjugation. *Adv. Mater.* **2018**, *30*, 1704713.
17. Li, T.; Dai, S.; Ke, Z.; Yang, L.; Wang, J.; Yan, C.; Ma, W.; Zhan, X. Fused Tris(Thienothiophene)-Based Electron Acceptor with Strong Near-Infrared Absorption for High-Performance As-Cast Solar Cells. *Adv. Mater.* **2018**, *30*, 1705969.
18. Ye, L.; Zhao, W.; Li, S.; Mukherjee, S.; Carpenter, J. H.; Awartani, O.; Jiao, X.; Hou, J.; Ade, H. High-Efficiency Nonfullerene Organic Solar Cells: Critical Factors That Affect Complex Multi-Length Scale Morphology and Device Performance. *Adv. Energy Mater.* **2017**, *7*, 1602000.
19. Zhang, J.; Yan, C.; Wang, W.; Xiao, Y.; Lu, X.; Barlow, S.; Parker, T. C.; Zhan, X.; Marder, S. R. Panchromatic Ternary Photovoltaic Cells Using a Nonfullerene Acceptor Synthesized Using C–H Functionalization. *Chem. Mater.* **2018**, *30*, 309–313.
20. Yang, L.; Gu, W.; Hong, L.; Mi, Y.; Liu, F.; Liu, M.; Yang, Y.; Sharma, B.; Liu, X.; Huang, H. High Performing Ternary Solar Cells through Förster Resonance Energy Transfer between Nonfullerene Acceptors. *ACS Appl. Mater. Interfaces* **2017**, *9*, 26928–26936.
21. Wang, W.; Yan, C.; Lau, T.-K.; Wang, J.; Liu, K.; Fan, Y.; Lu, X.; Zhan, X. Fused Hexacyclic Nonfullerene Acceptor with Strong Near-Infrared Absorption for Semitransparent Organic Solar Cells with 9.77% Efficiency. *Adv. Mater.* **2017**, *29*, 1701308.
22. Feng, H.; Qiu, N.; Wang, X.; Wang, Y.; Kan, B.; Wan, X.; Zhang, M.; Xia, A.; Li, C.; Liu, F.; et al. An A-D-A Type Small-Molecule Electron Acceptor with End-Extended Conjugation for High Performance Organic Solar Cells. *Chem. Mater.* **2017**, *29*, 7908–7917.
23. Hu, H.; Jiang, K.; Chow, P. C. Y.; Ye, L.; Zhang, G.; Li, Z.; Carpenter, J. H.; Ade, H.; Yan, H. Influence of Donor Polymer on the Molecular Ordering of Small Molecular Acceptors in Nonfullerene Polymer Solar Cells. *Adv. Energy Mater.* **2018**, *8*, 1701674.
24. Fan, Q.; Wang, Y.; Zhang, M.; Wu, B.; Guo, X.; Jiang, Y.; Li, W.; Guo, B.; Ye, C.; Su, W.; et al. High-Performance As-Cast Nonfullerene Polymer Solar Cells with Thicker Active Layer and Large Area Exceeding 11% Power Conversion Efficiency. *Adv. Mater.* **2018**, *30*, 1704546.
25. Chen, Y.; Ye, P.; Jia, X.; Gu, W.; Xu, X.; Wu, X.; Wu, J.; Liu, F.; Zhu, Z.; Huang, H. Tuning V Oc for High Performance Organic Ternary Solar Cells with Non-Fullerene Acceptor Alloys. *J. Mater. Chem. A* **2017**, *5*, 19697–19702.
26. Li, X.; Yan, T.; Bin, H.; Han, G.; Xue, L.; Liu, F.; Yi, Y.; Zhang, Z.-G.; Russell, T. P.; Li, Y. Insertion of Double Bond π-Bridges of A–D–A Acceptors for High Performance near-Infrared Polymer Solar Cells. *J. Mater. Chem. A* **2017**, *5*, 22588–22597.
27. Hexemer, A.; Bras, W.; Glossinger, J.; Schaible, E.; Gann, E.; Kirian, R.; MacDowell, A.; Church, M.; Rude, B.; Padmore, H. A SAXS/WAXS/GISAXS Beamline with Multilayer Monochromator. *J. Phys. Conf. Ser.* **2010**, *247*, 012007.